

Universal shape law of stochastic supercritical bifurcations: Theory and experiments

Gonzague Agez,¹ Marcel G. Clerc,¹ and Eric Louvergneaux²

¹*Departamento de Física, Facultad de Ciencias Físicas y Matemáticas, Universidad de Chile, Casilla 487-3, Santiago, Chile*

²*Laboratoire de Physique des Lasers, Atomes et Molécules, UMR-CNRS 8523, CERLA FR-CNRS 2416,*

Université des Sciences et Technologies de Lille, 59655 Villeneuve d'Ascq Cedex, France

(Received 26 July 2006; revised manuscript received 11 January 2008; published 26 February 2008)

A universal analytical expression for the supercritical bifurcation shape of transverse one-dimensional (1D) systems in the presence of additive noise is given. The stochastic Langevin equation of such systems is solved by using a Fokker-Planck equation, leading to the expression for the most probable amplitude of the critical mode. From this universal expression, the shape of the bifurcation, its location, and its evolution with the noise level are completely defined. Experimental results obtained for a 1D transverse Kerr-type slice subjected to optical feedback are in excellent agreement.

DOI: [10.1103/PhysRevE.77.026218](https://doi.org/10.1103/PhysRevE.77.026218)

PACS number(s): 05.10.-a, 45.70.Qj, 42.65.Hw

In nature, most physical systems are subjected to fluctuations. For a long time, the effects of these fluctuations were either considered as a nuisance (degradation of the signal-to-noise ratio) or ignored because it was not known how to handle them. For three decades, a wealth of theoretical and experimental research has shown that fluctuations can have rather surprisingly constructive and counterintuitive effects in many physical systems and that they can be figured out with the help of different analysis tools. These situations occur when there are mechanisms of noise amplification or when noise interacts with nonlinearities or driving forces on the system. The most well-known examples in zero-dimensional systems are noise-induced transition [1] and stochastic resonance [2]. More recently, examples of spatially extended systems are noise-induced phase transition, noise-induced patterns (see [3] and references therein), noise-sustained structures in convective instability [4], stochastic spatiotemporal intermittency [5], noise-induced traveling waves [6], noise-induced ordering transition [7], and front propagation [8]. Among these effects, a direct consequence of noise effects is the modification of the deterministic bifurcation shapes where the critical points and the physical mechanisms are masked by fluctuations. It is important to remark that the critical points generically represent a change of balance between forces. Hence, the characterization of noisy bifurcations is a fundamental problem due to the ubiquitous nature of bifurcations. For instance, the supercritical bifurcations transform into smooth transitions between the two states and the subcritical bifurcations experience hysteresis size modifications. In the absence of noise, the shape of a bifurcation and its characteristics are given by the analytical solution of the deterministic amplitude equation of the critical mode [9]. On the other hand, in the presence of noise, no such analytical expression can be obtained from the stochastic amplitude equation. In this latter situation, the below and above bifurcation point regimes are usually treated separately, but without continuity between their respective solutions. For instance, in noisy spatially extended systems in which the systems are characterized by the appearance of pattern precursors below the bifurcation point and by established patterns that fluctuate above this point [10], the pre-

cursor amplitude [11], obtained from the linear study of the stochastic equation, diverges at the bifurcation point and does not connect to the “mean” amplitude of the fluctuating pattern, obtained from the deterministic equation. To our knowledge, no universal analytical expression of the critical mode amplitude, describing the complete transition from below to above the bifurcation point, exists for the supercritical bifurcations in the presence of noise.

In this paper, we propose a universal description of the supercritical bifurcation shapes of one-dimensional (1D) transverse systems (either uniform or very slowly varying in space) in the presence of noise that is also valid for the second-order bifurcations of temporal (zero-dimensional) systems. *More precisely, we give a unified analytical expression for the most probable amplitude describing the supercritical bifurcations in the presence of noise, including the noise level and the deterministic bifurcation point location.* The systems under study are described by stochastic partial differential equations (SPDEs) of the Langevin type [12] (first order in time and with linear noise terms) involving additive white noise. First, we reduce the SPDE to an ordinary differential equation (ODE) for the amplitude of the critical mode. Second, we solve the Langevin ODE describing the stochastic dynamics by using a Fokker-Planck equation for the probability density of the critical mode amplitude. Then, from the stationary distribution of this amplitude, we deduce the bifurcation shape by means of the most probable value of the pattern amplitude. Finally, the comparison with experimental results obtained in a Kerr-type slice subjected to 1D optical feedback is given and leads to an excellent agreement.

Let us consider a 1D extended system that exhibits a supercritical spatial bifurcation described by

$$\partial_t \vec{u} = \vec{f}(\vec{u}, \partial_x \{\mu\}) + \sqrt{\eta_0} \vec{\zeta}(x, t), \quad (1)$$

where $\vec{u}(x, t)$ is a field that describes the system under study, \vec{f} is the vector field, $\{\mu\}$ is a set of parameters that characterizes the system, η_0 is the noise level intensity, and $\vec{\zeta}(x, t)$ is a white Gaussian noise with zero mean value and correlation $\langle \zeta^i(x, t) \zeta^j(x', t') \rangle = \delta^i j \delta(t' - t) \delta(x' - x)$.

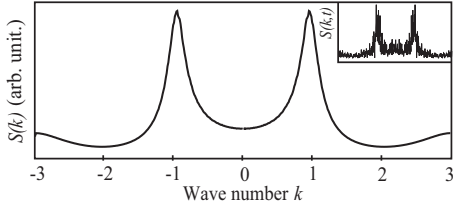


FIG. 1. Averaged Fourier transform modulus $S(k)$ of the field w for the supercritical Swift-Hohenberg equation (2) with $q=1$ obtained below the bifurcation point. The inset corresponds to an instantaneous snapshot of $S(k, t)$.

We assume that the associated deterministic system ($\eta_0=0$) possesses a stationary state \vec{u}_0 that satisfies $\vec{f}(\vec{u}_0, \partial_x, \{\mu\})=0$. Above a set of critical values $\{\mu_c\}$, the deterministic system exhibits a spatial instability such that \vec{u} reads $\vec{u}(x, t)=\vec{u}_0+e^{\lambda(k)t+ikx}\hat{u}_k$, where $\lambda(k)$ is the linear growth rate, k is the wave number of the instability, and \hat{u}_k is the eigenvector associated with this critical mode. Close to $\{\mu_c\}$, for $\lambda(k)<0$ (i.e., \vec{u}_0 is stable), the profile of λ already displays two maxima for non-null wave numbers close to the critical ones $\pm k_c$. Hence, below the bifurcation point, when noise is present, among all the excited spatial modes, the ones associated with the maximum growth rate ($k \approx \pm k_c$) will rule the dynamics. The dynamical behavior of the system will then be characterized by pattern precursors as illustrated in Fig. 1. It shows the instantaneous $S(k, t)$ and averaged $S(k)=\langle S(k, t) \rangle_t$ moduli of the Fourier transform of the field \vec{u} , also called the structure factor, for the supercritical Swift-Hohenberg equation [3] below the deterministic threshold. We can remark that the maxima of the function, both instantaneous and averaged, already give the incoming critical wave numbers $k_c = \pm 1$ (Fig. 1).

To describe the stochastic supercritical bifurcations of Eq. (1) type in a unified description close to the instability threshold, we consider the example of the stochastic supercritical Swift-Hohenberg model [3] for pattern formation which reads

$$\partial_t w = \mu w - w^3 - (\partial_{xx} + q^2)^2 w + \sqrt{\sigma_0} \zeta(x, t), \quad (2)$$

where $w(x, t)$ is in general a real field. $\mu - q^4$ is the bifurcation parameter, q is the transverse wave number of periodical solutions, $\zeta(x, t)$ is a Gaussian white noise with zero mean value and correlation $\langle \zeta(x, t) \zeta(x', t') \rangle = \delta(x - x') \delta(t - t')$, and σ_0 represents the intensity of noise. A trivial uniform stationary state of the deterministic model of Eq. (2) is $w(x, t) = 0$. This state is stable for $\mu < 0$ and exhibits a supercritical spatial instability for $\mu = 0$, which gives rise to the appearance of a pattern for $\mu > 0$. In order to describe the appearance of pattern formation, we consider the small bifurcation parameter ε such that $\varepsilon = \mu \ll 1$. The transverse domain of the system is taken to be finite, of size L , and for the sake of simplicity we consider periodic boundary conditions $w(x = -L/2, t) = w(x = L/2, t)$. To capture the dynamics of Eq. (2) we introduce the ansatz

$$w = \frac{a(T)}{\sqrt{3}} e^{iqx} + \frac{\bar{a}(T)}{\sqrt{3}} e^{-iqx} + U(a, \bar{a}, x), \quad (3)$$

where $q \approx 2\pi n/L$ for wide enough L , $a(T)$ is the space-independent amplitude of the critical mode q , and $U(a, \bar{a}, x)$ is a small correction function including high-order terms in a, \bar{a} . This ansatz is restricted to the single amplitude $a(T)$ of the most unstable wave vector $q \equiv k_c$. It is clear that to describe the full spatial variation of $a(x, T)$ we should consider more critical wave vectors as shown in Refs. [13, 14]. However, in this paper, we derive in a first step an analytical expression of the most probable value of $a(T)$. We will show, with the help of numerical simulations, that the plot of the most probable value of $a(x, T)$ is in very good agreement with the one of the most probable value of $a(T)$ based on a single wave vector approximation. The “taking into account” of more wave vectors would lead to a functional amplitude for the stationary probability density of a and is out of the scope of this paper. Work in this direction is in progress.

The amplitude a , slow time $T = \varepsilon t$, and $U(a, \bar{a}, x)$ are of the order of $\varepsilon^{1/2}$, ε , and ε^3 , respectively. Introducing the ansatz (3) into Eq. (2), we obtain at order ε^3

$$\begin{aligned} (\partial_{xx} + q^2)^2 U = \{ -\partial_T a + \varepsilon a - |a|^2 a \} \frac{e^{iqx}}{\sqrt{3}} - \frac{a^3}{3\sqrt{3}} e^{-i3qx} \\ + \sqrt{\sigma_0} \zeta(x, t) + \text{c.c.}, \end{aligned} \quad (4)$$

where “c.c.” means “complex conjugate.” The linear operator $(\partial_{xx} + q^2)^2$ is a self-adjoint with inner product $\langle f | g \rangle = \frac{1}{L} \int_{-L/2}^{L/2} f \bar{g}$, and it is not invertible because $(\partial_{xx} + q^2)^2 e^{\pm iqx} = 0$. In order to have solutions for U , we multiply the right-hand side of Eq. (4) by e^{-iqx}/L , integrate in whole domain, and impose that it be equal to zero (Fredholm alternative or solvability condition). Hence, we obtain the amplitude equation

$$\partial_T a = \varepsilon a - |a|^2 a + \sqrt{\eta} \xi(T), \quad (5)$$

where $\eta = 3\sigma_0$ and

$$\xi(T) \equiv \frac{1}{L} \int_{-L/2}^{L/2} \zeta(x, T) e^{-iqx} dx,$$

with correlation $\langle \xi(T) \xi(T') \rangle = 0$ and $\langle \xi(T) \bar{\xi}(T') \rangle = \delta(T' - T)$. It is important to note that the dynamics close to supercritical spatial bifurcation is described by Eq. (5) [9].

The general way of obtaining a solution of the Langevin equation (5) is by use of a Fokker-Planck equation which provides us with a deterministic equation satisfied by the time-dependent probability density $P(a, \bar{a}; T)$ [12] of the amplitude a , which reads

$$\partial_T P = \partial_a \left\{ -\varepsilon a + |a|^2 a + \frac{\eta}{2} \partial_{\bar{a}} \right\} P + \text{c.c.} \quad (6)$$

The associated stationary probability density of the modulus of a is

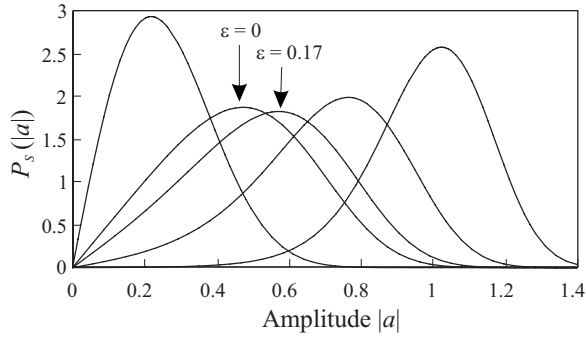


FIG. 2. Stationary probability distribution $P_s(|a|)$ for different values of the bifurcation parameter ε . From left to right, $\varepsilon = -1, 0, 0.17, 0.5, 1$. $\eta = 0.1$.

$$P_s(|a|, \varepsilon, \eta) = Q(\varepsilon, \eta) |a| e^{[\varepsilon |a|^2 - (|a|^4/2)/\eta]}, \quad (7)$$

where $Q(\varepsilon, \eta) \equiv 2\sqrt{2}e^{-\varepsilon^2/2\eta}/\text{erfc}(-\frac{\varepsilon}{\sqrt{2}\eta})\sqrt{\pi\eta}$. This stationary probability density is shown in Fig. 2 for different values of the bifurcation parameter ε . The probability density function is not symmetrical with respect to its maximum so that the most relevant quantity for characterizing $P_s(|a|, \varepsilon, \eta)$ is its maximum and not its mean value as usually calculated, e.g., in experiments. The value of $|a|$ corresponding to the maximum of $P_s(|a|, \varepsilon, \eta)$ occurs at the expectation value $|a_{\max}|$ given by

$$|a_{\max}| = \sqrt{\frac{\varepsilon + \sqrt{\varepsilon^2 + 2\eta}}{2}}. \quad (8)$$

The comparison of this analytical expression with the numerical simulations performed on Eq. (5) is depicted in Fig. 3. It clearly shows a very good agreement between the numerical values of $|a_{\max}|$ obtained from the numerical simulations of the stochastic supercritical Swift–Hohenberg equation (2) and its analytical values [formula (8)]. Thus, the plot of $|a_{\max}|$ gives the searched for supercritical bifurcation

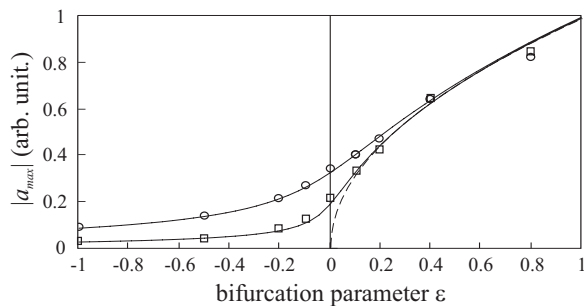


FIG. 3. Influence of the noise level η on the shape of the imperfect supercritical bifurcation. The squares and circles are obtained from the numerical simulations of the stochastic Swift–Hohenberg equation (2) with $q=1$ and a noise intensity, respectively, $\sigma_0=0.001$ and $\sigma_0=0.01$. The solid curves correspond to the analytical expectation value $|a_{\max}|$ of Eq. (8); the corresponding mean-square fit values are $\eta^{(fit)}=0.0035$ and $\eta^{(fit)}=0.032$ (in accordance with the relation $\eta=3\sigma_0$).

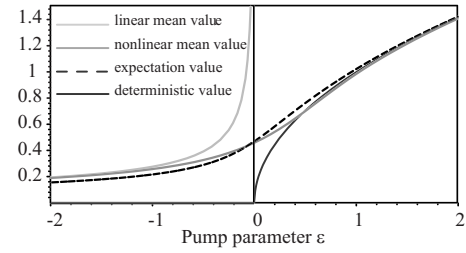


FIG. 4. Bifurcation diagrams of the amplitude of the critical mode obtained for different solutions of Eq. (5)—namely, the deterministic value, the expectation value $|a_{\max}|$, and the linear and nonlinear mean values $\langle |a| \rangle_{\text{linear}}$ and $\langle |a| \rangle_{\text{nonlinear}}$, respectively (see text for value definitions).

shape in the presence of noise. As this latter expression includes the noise level η , we can easily follow the continuous deformation and evolution of the bifurcation shape with the level of noise as can be seen in Fig. 3. Finally, when the bifurcation parameter ε is driven far from 0 ($|\varepsilon| \gg 1$), this expectation value converges to zero ($\sqrt{-\eta/2\varepsilon}$) for negative values of ε and to $\sqrt{\varepsilon}$ for positive values, then coinciding exactly with the values of the amplitude a for the deterministic case of Eq. (5). Thus, the expression of $|a_{\max}|$ is the relevant one to describe the noisy supercritical bifurcations including the noise level and the bifurcation point location ($\varepsilon=0$) of systems satisfying Eq. (1).

Let us now discuss the choice of $|a_{\max}|$ for describing the noisy supercritical bifurcation against other quantities such as, for instance, the averaged value of a . If we neglect the nonlinear term in the Langevin equation (5), one can perform a linear stability analysis that provides us with the linear mean value of the amplitude modulus, $\langle |a| \rangle_{\text{linear}} = \sqrt{-\pi\eta/4\varepsilon}$. Note that this value diverges at the bifurcation point and is only valid for $\varepsilon < 0$ (Fig. 4). The nonlinear mean value $\langle |a| \rangle_{\text{nonlinear}}$ is computed numerically from the time average of a . All the linear mean, nonlinear mean, expected, and deterministic values of the critical mode amplitude are reported in Fig. 4 for comparison. The interesting region is located in the vicinity of the bifurcation point ($\varepsilon=0$) where the behaviors of the different curves strongly differ. The linear mean value and the deterministic value do not correspond to a realistic physical behavior since the amplitude never diverges at threshold and we are considering a noisy system respectively. Only the nonlinear mean and expected values can mimic the supercritical bifurcation in presence of noise. However, as we have mentioned earlier, due to the asymmetry of $P_s(|a|, \varepsilon, \eta)$, the most probable and relevant value for describing the evolution of the amplitude versus the control parameter is the expectation value $|a_{\max}|$.

Regardless of the sign of ε , the width of the stationary probability distribution decreases as $|\varepsilon|$ increases far from 0 (Fig. 2). It is maximum when ε corresponds to a change in the dynamics of the system. The dynamics is then characterized by large amplitude fluctuations coinciding with a minimum of $P_s(|a_{\max}|)$ versus ε . In the case of Fig. 5 this *intrinsic bifurcation point* occurs at $\varepsilon_{\min} \approx 0.1$ which is shifted from the deterministic bifurcation point $\varepsilon=0$. This shift reminds us of bifurcation postponements as in [15]. A straightforward calculation gives

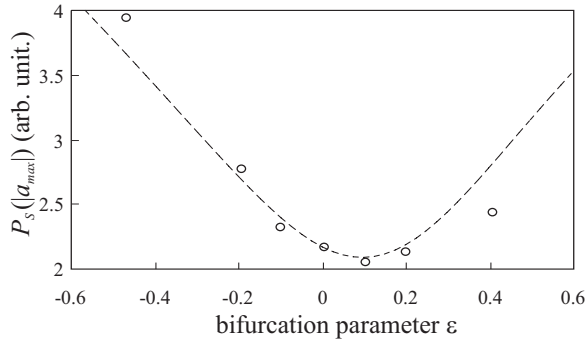


FIG. 5. Evolution of $P_s(|a_{\max}|)$ versus ε for $\eta=0.03$ ($\sigma_0=0.01$) showing a minimum at the intrinsic bifurcation point $\varepsilon_{\min} \approx 0.1$.

$$\varepsilon_{\min}(\eta) \approx 0.55\sqrt{\eta}.$$

Thus, the plot of $P_s(|a_{\max}|)$ provides us with the intrinsic bifurcation point location which corresponds to the relevant location for the change in the dynamical regime of the stochastic system.

In addition to the very good agreement between the analytical expression of $|a_{\max}|$ and the numerical simulations, we checked the assumption on the restriction to the single most unstable wave vector $q \equiv k_c$ in the ansatz (3). We performed a space and time extraction of the critical mode amplitude $a(x, T)$ by the well-known Hilbert transformation. We got for each time T the spatial profile $a(x, T)$ [Fig. 6(c)] of $w(x, T)$

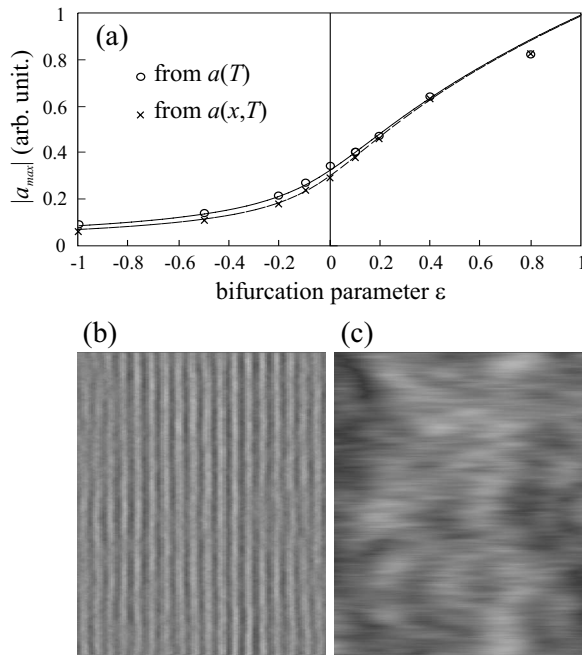


FIG. 6. (a) Comparison of the stochastic bifurcation shapes obtained from a space-independent amplitude $a(T)$ [Eq. (3)] and from a space-dependent amplitude $a(x, T)$ for $\eta=0.03$. (b) Spatial evolution of $w^2(x, T)$ versus time T and (c) its corresponding amplitude $a(x, T)$. Space and time are, respectively, the horizontal and vertical axes.

[Fig. 6(b)]. Then, we plotted the stationary probability densities to extract the corresponding values of the expectation value $|a_{\max}|$. Figure 6(a) depicts the stochastic bifurcation then obtained from $a(x, T)$ together with that obtained from $a(T)$. The two shapes give quite the same values of η : 0.032 with the first method and 0.028 with the Hilbert treatment. Thus, the single wave vector approximation in the ansatz (3) is a good assumption and the analytical expression of $|a_{\max}|$ is relevant to describe the shape of the SPDE (2).

In order to completely validate the universal law of Eq. (8), we have applied our analysis to experiments realized on a noisy 1D transverse system known to exhibit a supercritical bifurcation at the onset of roll pattern formation. The system is a nematic liquid-crystal (LC) slice subjected to optical feedback (cf. inset of Fig. 8) based on the well-known feedback optical system [16,17]. The corresponding stochastic model reads [4]

$$\partial_t u = (\partial_{xx} - 1)u + |F|^2 + R|e^{i\sigma\partial_{xx}}(e^{i\chi u}F)|^2 + \sqrt{\eta_0}\zeta, \quad (9)$$

where $u(x, t)$ stands for the refractive index of the nonlinear nematic LC layer, t and x are the time and transverse space variables scaled with respect to the relaxation time τ and the diffusion length l_d , and R is the mirror intensity reflectivity. $\sigma=d/k_0$ where d is the slice-mirror distance and k_0 is the optical wave number of the field. F is the forward input optical field; its transverse profile is accounted for using $F(x)=F_0 \exp(-x^2/w^2)$ for a Gaussian pump beam of radius w . ζ and η_0 are the noise source and level, respectively, as defined in Eq. (1). The Kerr effect is parametrized by χ which is positive (negative) for a focusing (defocusing) medium.

Equation (9) is similar to Eq. (1) and leads to an amplitude equation [Eq. (24) in Ref. [18]] which is the same as the deterministic part of Eq. (5). The spatial variations of the pumping beam around its maximum are slow (less than 10% for a domain width L including fewer than ten rolls) due to the high transverse aspect ratio ($2wk_c/2\pi \geq 30$). Thus, the conditions are fulfilled to apply the previous analysis to our experimental noisy system in order to describe its supercritical bifurcation. Figure 7 shows probability density functions calculated from experimental spatiotemporal diagrams for a transverse domain width L around the center of the Gaussian pumping beam. In Fig. 8 we have plotted the experimental recordings of the amplitude expectation value $|a_{\max}|$ together with its analytical expression [Eq. (8)]. We can see that the analytical expression fits very well the experimental values. It provides us with the deterministic threshold $I = 151 \text{ W cm}^{-2}$. The intrinsic bifurcation point ε_{\min} could not be located from $P_s(|a_{\max}|)$ since this latter does not depict a clear minimum due to the Gaussian profile of $F(x)$. The analysis was performed on many regions of spatial width L ranging from very limited transverse extensions close to the center of the pump profile to the full width of the transverse profile. The results always led to the same bifurcation shape. So the universal amplitude expression of Eq. (8) is valid and relevant to describe the supercritical spatial bifurcation shape of our noisy system and more generally to describe the su-

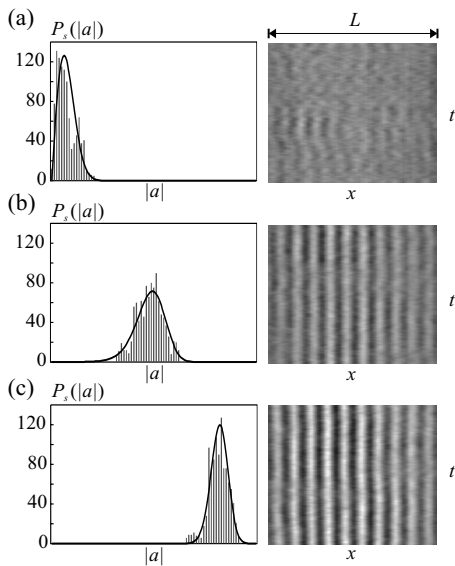


FIG. 7. Right: Spatiotemporal diagrams built from experimental roll patterns. Left: Experimental probability amplitude histograms and corresponding probability density functions [Eq. (7)]. (a) $I = 108 \text{ W/cm}^2$, (b) $I = 154 \text{ W/cm}^2$, and (c) $I = 180 \text{ W/cm}^2$.

percritical bifurcations of 1D systems in presence of noise even with nonuniform transverse profiles, assuming that they vary very slowly in space.

In conclusion, we have given an universal amplitude equation for 1D systems in the presence of noise. From this equation, we have derived an analytical expression for the

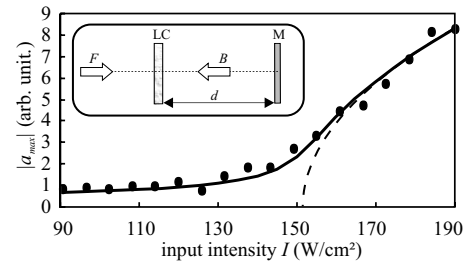


FIG. 8. Experimental bifurcation diagram for the optical feedback system. The dots are the experimental measured values of $|a_{\max}|$ and the solid curve its fitted analytical value [Eq. (8)]. The dashed line is the corresponding deterministic bifurcation deduced from the fit. The inset is a schematic sketch of the experimental setup. LC, liquid-crystal layer; M, feedback mirror; F, input optical field; B, backward optical field; d , feedback length.

amplitude expectation value that fully describes the noisy supercritical bifurcations. The agreement with experiments carried out for a 1D pattern-forming system is excellent. This amplitude equation can be applied to any second-order transition of noisy temporal systems.

We thank Rene Rojas for useful discussions. The simulation software DIMX developed at the laboratory INLN in France has been used for some numerical simulations. We thank for support Anillo Grant No. ACT15, FONDAPE Grant No. 1020374, and the ECOS-Sud Committee. The CERLA is supported in part by the ‘‘Conseil Regional Nord Pas de Calais’’ and the ‘‘Fonds Europeen de Developpement Economique des Regions.’’

-
- [1] W. Horsthemke and R. Lefever, *Noise-induced Transitions: Theory and applications in physics, chemistry and biology* (Springer, Berlin, 1984).
- [2] L. Gammaitoni, P. Hanggi, P. Jung, and F. Marchesoni, *Rev. Mod. Phys.* **70**, 223 (1998).
- [3] J. Garcia-Ojalvo and J. M. Sancho, *Noise in Spatially Extended Systems* (Springer-Verlag, New York, 1999).
- [4] G. Agez, P. Glorieux, M. Taki, and E. Louvergneaux, *Phys. Rev. A* **74**, 043814 (2006).
- [5] M. G. Zimmermann, R. Toral, O. Piro, and M. San Miguel, *Phys. Rev. Lett.* **85**, 3612 (2000).
- [6] L. Q. Zhou, X. Jia, and Q. Ouyang, *Phys. Rev. Lett.* **88**, 138301 (2002).
- [7] R. Muller, K. Lippert, A. Kuhnel, and U. Behn, *Phys. Rev. E* **56**, 2658 (1997).
- [8] M. G. Clerc, C. Falcon, and E. Tirapegui, *Phys. Rev. Lett.* **94**, 148302 (2005); M. G. Clerc, C. Falcon, and E. Tirapegui, *Phys. Rev. E* **74**, 011303 (2006).
- [9] M. C. Cross and P. C. Hohenberg, *Rev. Mod. Phys.* **65**, 851 (1993) and references therein.
- [10] G. Agez, C. Szwaj, E. Louvergneaux, and P. Glorieux, *Phys. Rev. A* **66**, 063805 (2002).
- [11] W. Schopf and W. Zimmermann, *Phys. Rev. E* **47**, 1739 (1993).
- [12] N. G. Van Kampen, *Stochastic Process in Physics and Chemistry* (North-Holland, Amsterdam, 1992).
- [13] M. N. Ouarzazi, P. A. Bois, and M. Taki, *Phys. Rev. A* **53**, 4408 (1996).
- [14] P. C. Hohenberg and J. B. Swift, *Phys. Rev. A* **46**, 4773 (1992).
- [15] R. Lefever and J. W. Turner, *Phys. Rev. Lett.* **56**, 1631 (1986).
- [16] S. A. Akhmanov, M. A. Vorontsov, and V. Yu. Ivanov, *JETP Lett.* **47**, 707 (1988); S. A. Akhmanov, M. A. Vorontsov, V. Yu. Ivanov, A. V. Larichev, and N. I. Zheleznykh, *J. Opt. Soc. Am. B* **9**, 78 (1992).
- [17] W. J. Firth, *J. Mod. Opt.* **37**, 151 (1990).
- [18] G. D’Alessandro and W. J. Firth, *Phys. Rev. A* **46**, 537 (1992).